International Journal of Applied Engineering Research
ISSN 0973-4562 Volume 10, Number 12 (2015) pp. 31233-31248

http://www.ripublication.com

Crash Testing Of Self Piercing Rivet Using Ls Dyna Software

[1]Mathew Alphonse, [2]R.Ganesh, [3]N.Murugu Nachippan, [4]V.Vennishmuthu

[1, 2]Assistant professor,
Department of Mechanical Engineering, Veltech University, Chennai,
Tamil Nadu, India
[3,4]Assistant professor,
Department of Automobile Engineering, Veltech University, Chennai,
Tamil Nadu, India
[1]gnmathew@gmail.com, [2]ganeshr_07@rediffmail.com com,
[3]murugunachippan@gmail.com, [4]vennish1990@gmail.com

Abstract

Self-piercing riveting (SPR) is a process of joining two pieces of material using a rivet. Unlike conventional riveting, self-piercing riveting does not require a pre-drilled hole, because the rivet creates its own hole as it is being inserted. This makesself-piercing rivet is good in terms of production cost reduction and ease of use compared to conventional riveting. The practice of coated, lightweight and high-strength materials, such as galvanized or pre-painted steel and aluminium is increased which has steered industries to re-examine conventional methods of assembling components. The value of a self-piercing rivet that syndicates high joint integrity with rapid assembly times that become obvious because welding of these materials is challenging or difficultand assembly using conventional rivets is slow and costly.A self-piercingrivet jointsample is studied. The sample consists of 4 mm thick sheets with a rivet of 8 mm in waist-diameter. The finite element software LS-Dyna /Explicit, and involve dynamic inertia effects is used for the simulation. The Johnson-Cook plasticity model is used to describe the materials, Mat 20 and Mat 24 ie., Mat 20 denotes Rigid Material and Mat 24 denotes Piecewise Linear Isotropic Plasticity. The results are gathered and assembled to energy-curves and velocity-curves.

Keywords: Crash testing, Self-piercing rivet, LS-Dyna /Explicit, Energy-curves, Velocity-Curves.

1. Introduction

In recent scenario of automotive industry, companies save more amount of money through simulations. The computer simulations are used for example to test crashworthiness, with aobjective to increase the safety in cars. Basically all phenomena, which describe a process that involves some kind of variation, can be described by means of differential equations. Mathematics becomes then the natural means to understand and describes such a phenomenon, and to interpret and solve them. Effective and reliable numerical models are necessary to be capable to optimize, weight, production cost and structural strength.

The joints that join different parts in a car body are often the weakest points as regards to structural strength. They can break due to fatigue or by extreme forces, like a crash. A car body contains many joints, so a full car model must be simple enough to give reasonable demands on the computer's memory and speed.

The finite element method is today the most widely used technique for computer based analysis of problems within mechanics of materials. The method started to develop in the 50's and has developed ever since.

Today it is possible to analyse three – dimensional geometry with consideration of both large deformations and non- linear material behaviour, finite element calculations are performed using the software LS DYNA/ Explicit.Crash testing leads to improvement of the safety systems. These systems again have to be tested for their workability during a crash. Hence crash testing plays a vital role in continuous improvement of the safety systems. It is reported that SPR beams decrease as the material densities of the sheets increases. The natural frequency ratios of the torsional modes decrease as material densities of sheets increases [1]. The specific density of magnesium alloys materials, which is approximately two-third that of aluminum alloy materials has a lower environmental effect when used in casting and die-casting processes [3].LS-DYNA hourglass formulations pass the 3D Patch Test, and provides sufficient details of the patch test to allow readers to repeat the test [6].

One of the key components in the new SAFER barrier being fitted at many IRL and NASCAR racetracks is the foam blocks placed between an outer steel tube structure and the existing concrete wall. Successfully modeling of the foam, as described in this paper, has played an important role in the development of the SAFER barrier [7]. The frontal crash of the integrated car system is effectively simulated in LS-DYNA and the results that including the structures' section forces and energy absorption time courses, the result of the main energy-absorbing parts, the transmitting route of the energy and the forces change are attained. The numerical Simulation effects show, the structures' section forces can accurately forecast not only crashworthiness of vehicles but also the way transmission of forces in crash process. This technique provides an important tool to improve vehicle's structures' performances[10].Subsequently Self-piercing rivets (SPR) are becoming more and more common as joining methods in cars for frame structures of aluminium, It is important that the rivet joints don't separate while submitted to crash load so that an unstable collapse of the car body structure can be avoided.

2. Requirements of Joint

In order to have aacceptable rivet joint, the requirements detailed below must be complied with. The requirements apply to each individual self-piercing rivet in the joint.

2.1 Punch side

1. The surface of the rivet head shall be parallel with the sheet metal surface.
2. In the case of countersunk rivets, the rivet head may be max. 0.2 mm above the sheet metal surface.
3. In the case of countersunk rivets, the rivet head may be max. 0.1 mm below the sheet metal surface.

2.2 Die side

1. A fully shaped button shall show an outer diameter corresponding to the inside dimension of the die tool.
2. No breakthrough of the rivet permitted.
3. No cracks in the sheet permitted.
4. The remaining sheet thickness shall be min 0.2 mm.

3. Details of Analysis

The sheets are 2 mm thick. The total length of the sample is 20 mm, and the height is 5 mm. The total width of the model is 15 mm butthe rivet has a head-diameter of 5 mmand waist-diameter of 4 mm. The dimensions are chosen according to other reports on crash. For the final geometry model, see Figure 1 &2 for an overview.

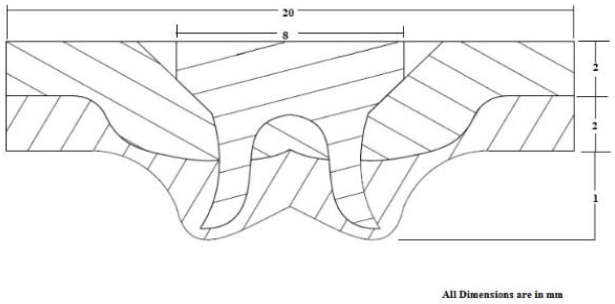

Fig.1. Self-piercing rivet

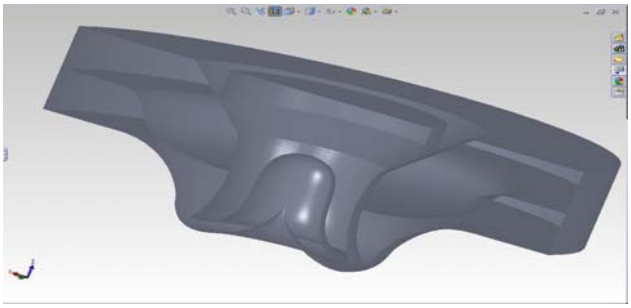

Fig.2.Cut Section Self -Piercing Rivet

The geometry of the rivet region done and it is imported to LS Dyna /Explicit.

LS-DYNA is a general purpose finite element code for analyzing the large deformation static and dynamic response of structures including structures coupled to fluids. The keysolution methodology is based on explicit time integration.

3.1 Central difference method

The explicit time integration method used in LS DYNA is the central difference method. The equilibrium is expressed at an instant when the displacements are identified. By means of this information, new equilibrium data can be calculated for the next time step.

The suggestion of the method is that known information between the previous time step and the current are used to calculate the equilibrium at current time step.

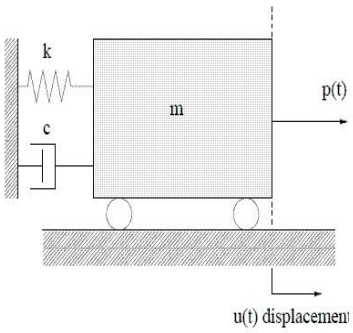

Fig.3. Single DOF with damper

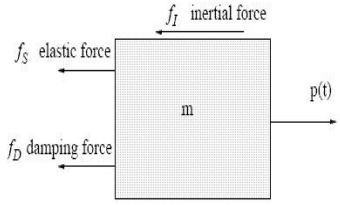

Fig.4. Forces acting on mass m

3.2 Equilibrium - d Alembert s principle

$f_I + f_D + f_S = p(t)$

Inertia force : $f_I = m\ddot{u}\ddot{u} = \frac{d^2y}{dt^2}$ - acceleration

Viscous damping: $f_D = c\dot{u}\dot{u} = \frac{du}{dt}$ - velocity

Linear elasticity : $f_S = ku$ u- displacement

The equation of motion for linear elasticity is

$m\ddot{u} + c\dot{u} + ku = p(t)$

3.3 Direct Integration of Equation of Motion

1. For nonlinear problems only numerical solutions are possible.
2. Focus is on explicit methods, in particular Central Difference method.
3. LS-DYNA uses a modification of the central difference time integration.
4. Central difference scheme is an explicit method.
5. For explicit schemes the equation of motion is evaluated at the old time step t_n, whereas implicit methods use the equation of motion at the new time step t_{n+1}.

3.4Johnson Cook plasticity model

Computer simulations have been in use for decades in the modeling of hypervelocity impacts and general large deformation problems. The variety of geometric configurations and for any number of materials the computer codes have been developed to simulate that problem.

These codes make use of several constitutive material models to simulate the response of the material under a variety of thermo-mechanical conditions..

In the Johnson-Cook constitutive model, describe the flow stress as the product of strain, strain rate and temperature effect namely work hardening, strain-rate hardening, and thermal softening

$$\bar{\sigma} = \lfloor A + B \rfloor . \varepsilon_{pl}^{n} \left[1 + C \ \ln\left(\frac{\dot{\varepsilon}_{pl}}{\dot{\varepsilon}_0}\right) \right] . \left(1 - \hat{\theta}^m\right)$$

σ =yield stress (P_a)

A= initial yield stress at $\dot{e}_0$ (P_a)

B= strain hardening coefficient

$\bar{e}$ = effective plastic strain

n = strain hardening exponent
C = strain rate- hardening coefficient
$\dot{\varepsilon}_{pl}$ = time derivative of effective plastic strain
$\dot{\varepsilon}_0$ = reference strain rate sensitivity constant

The stresses and strain refer to von mises effective values.

The parameter *A* is the initial yield strength of the material at room temperature. The corresponding plastic strain rate ε is normalized with a reference strain rate $\dot{e}$. The Johnson- Cook model is a well-accepted and numerically robust constitutive material model and highly utilized in modelingand simulation studies. The Johnson-Cook (JC) model assumes that the slope of the flow stress curve is independently affected by strain hardening, thermal softening and strain rate sensitivity behaviors. Each of these sets is indicated by the brackets in the constitutive equation. Several researchers have conducted split Hopkinson pressure bar (SHPB) high speed compression tests to obtain the parameters *A*, *B*, *C*, *n* and *m* of the constitutive equation by fitting the experimental data as given.

The Conducted high compression tests and determined constants for JC by using a computer program which performed an optimization routine to fit the experimental data. They have also used a parameter indicating the degree of fit defined

$$\delta = \frac{1}{n}\sum_{i=1}^{n}\frac{\sigma_{calculated}(\epsilon_i) - \sigma_{experimental}(\epsilon_i)}{\sigma_{experimental}(\epsilon_i)}$$

Table 1: Constants for the Johnson-Cook constitutive model

	AISI 1045 steel	AISI 4340 Steel	AL 6082-T6 aluminium	Ti 6A14V Titanium	Ti 6A14V Titanium
A	553.1	2100	428.5	782.7	896
B	600.8	1750	327.7	498.4	656
C	0.013	0.0028	0.00747	0.028	0.0128
N	0.234	0.65	1.008	0.28	0.50
M	1	0.75	1.31	1.0	0.8
T (K)	1733	1783	855	1933	1933

3.5 Input data Finite Element Model

3.5.1 Mesh Details

Simulations of crash testing normally give large deformations, which can give distorted Elements. When elements become distorted the calculation time increases due to the explicit procedure and in the worst case the calculation can be prevented. Mesh type used was tria. Total area 900 and volume 1423.81, Mesh consists of 32, 692 elements and 9402 nodes.

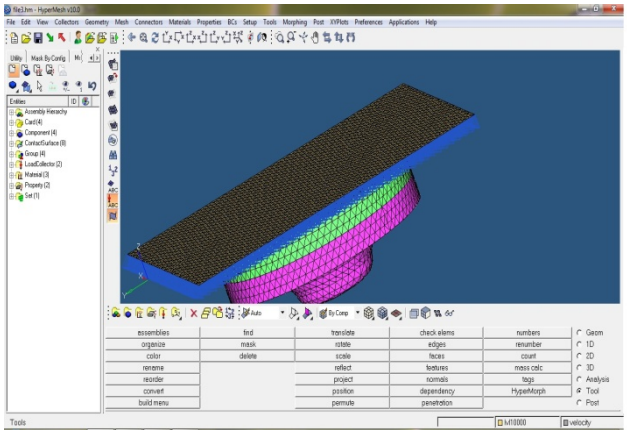

Fig.5.Meshed Specimen

3.5.2 Material Properties

Self-Piercing Rivet Consists of Head, Rivet, Plate 1, and Plate 2. Material to be assumed to have Elasto – plastic Response, Materials are isentropic. Material used are Mat 20 and Mat 24, Mat 20 for wall and Mat 24 for Plate1, Plate 2, head and rivet. Mat 20 is rigid and Mat 24 is Piecewise Linear Isotropic Plasticity.In the table below, a list of the available material models and the applicable element types are given.

Table 2: Applicable element type

Material Model	Mat 20	Mat 24
Material Name	Elastic	Piecewise linear Plasticity
Brick	Y	Y
Beam	Y	Y
Thin shell	Y	Y
Thick Shell	Y	Y
Strain- Rate Effect		Y
Failure		Y
Thermal Effect		
Material Type	General	Metal Plastic

3.5.3Material Type 20: Rigid

The Rigid material type 20 provides a convenient way of turning one or more parts comprised of beams, shells, or solid elements into a rigid body. Approximating a deformable body as rigid is a preferred modeling technique in many real world applications. For example, in sheet metal forming problems the tooling can properly and accurately be treated as rigid.

In the design of restraint systems the occupant can, for the purposes of early design studies, also be treated as rigid. Elements which are rigid are bypassed in the

element processing and no storage is allocated for storing history variables; consequently, the rigid material type is very cost efficient.

Two unique rigid part IDs may not share common nodes unless they are merged together using the rigid body merge option. A rigid body may be made up of disjoint finite element meshes, however.

LS-DYNA assumes this is the case since this is a common practice in setting up tooling meshes in forming problems.

All elements which reference a given part ID corresponding to the rigid material should be contiguous, but this is not a requirement. If two disjoint groups of elements on opposite sides of a model are modeled as rigid, separate part ID's should be created for each of the contiguous element groups if each group is to move independently.

This requirement arises from the fact that LS-DYNA internally computes the six rigid body degrees-of-freedom for each rigid body (rigid material or set of merged materials), and if disjoint groups of rigid elements use the same part ID, the disjoint groups will move together as one rigid body.

Inertial properties for rigid materials may be defined in either of two ways. By default, the inertial properties are calculated from the geometry of the constituent elements of the rigid material and the density specified for the part ID. Alternatively, the inertial properties and initial velocities for a rigid body may be directly defined, and this overrides data calculated from the material property definition and nodal initial velocity definitions.

Young's modulus, E, and Poisson's ratio, υ are used for determining sliding interface parameters if the rigid body interacts in a contact definition. Realistic values for these constants should be defined since unrealistic values may contribute to numerical problem in contact.

3.5.4 Material Type 24 : Piecewise Linear Isotropic Plasticity

This plasticity treatment in this model is quite similar, it includes strain rate effects and does not use an equation of state.

Deviatoric stresses are determined that satisfy the yield function

$$\emptyset = \frac{1}{2} s_{ij} s_{ij} - \frac{\sigma_y^2}{3} \leq 0$$

Where

$$\sigma_y = \beta[\sigma_0 + f_h(\varepsilon_{of}^p)]$$

Where the hardening function $f_h(\varepsilon_{of}^p)$ can be specified in tabular form as an option.For shell element, the above equations apply, but with the addition of an iterative loop to solve for the normal strain increment, such that the stress component normal to the mid surface of the shell element approaches zero.

Three options to account for strain rate effects are possible:

1. Strain rate may br accounted for using the Cowper – Symonds model which scales the yield stress with the factor

$$\beta = 1 + \left(\frac{\dot{\varepsilon}}{C}\right)^{1/p}$$

Where $\dot{\varepsilon}$ is the stain rate.

2. For complete generality a load curve, defining β, which scales the yield stress may be input instead. In this curve the scale factor versus stain rate is defined.

A fully visco plastic formulation is optional which incorporates the different options above within the yield surface. An additional cost is incurred over the simple scaling but the improvement is results can be dramatic.

Effective plastic strain versus yield stress is expected. If the strain rate values fall out of range, extrapolation is not used; rather, either the first or last curve determines the yield stress depending on whether the rate is low or high, respectively.

Steps

1. Contact surface is created between each ie., between plate 1 and plate 2, plate 1 and head, plate2 and head. Card image as set segment. Contact Surface created is to transfer load between plate 1, plate2, head and rivet.
2. Interfaces is use to assign contact, that we created already. Plate 1 to plate2, plate 2 to head, plate1 to head.
3. Create contact between plate and wall.
4. Assign contact between plate and wall
5. Material for for wall is specified as Mat 20 rigid. Material for plate, plate2, rivet and head as Mat 24 Piecewise Linear Isotropic Plasticity.
6. Property for plate1, plate2, rivet and head as solid. ELForm (Element Formation) given as 10, for wall given as shell thickness of 1mm, ELForm given as 3mm.
7. Load is applied on self piercing rivet which cause to hit on rigid wall.
8. Several control cards are applied ie., End time -1, D3 plot -0.01, Time step – 0.01, Data base option, RC Force – 0.1, SLE Out -0.1, Matsum – 0.1, GL Stat -0.1, El Out – 0.1.

3. Results from Finite element simulation

In this chapter the influence of different parameters are evaluated and discussed. A summary of the result from the simulations are shown. Due to oscillation of the curves it is not easy, in some cases; to see exactly were failure occurs. Failure is defined as the instant of complete separation of the parts in the model. The loads reported were obtained by summation of the reaction forces at the right-hand border and combining these with the corresponding displacement. The results are multiplied by two to get the result for the whole model. This gives the load-displacement curves,

from which the failure displacement, peak load and maximum load after oscillation are extracted.

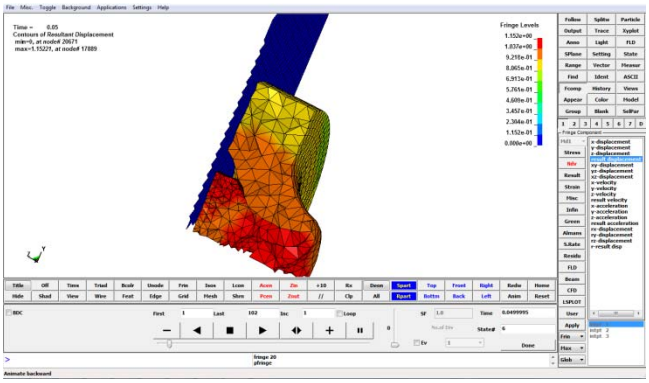

Fig.6. Contours of Resultant Displacement

Fig.6. represents a plots from LS- Dyna, showing the resultant displacement. The joint is disintegrated by the top-sheet peeling itself over the rivet. For the resultant displacement cases the blank part is removed to get a better view of the rivet. The blank part takes practically no stress.

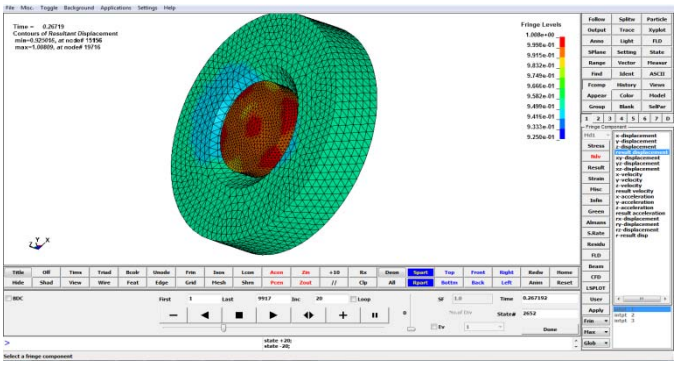

Fig.7. Contours of Resultant Displacement

Fig.7. represents a plots from LS- Dyna, showing the resultant displacement. The joint is disintegrated by the top-sheet peeling itself over the rivet. For the resultant velocity cases the blank part is removed to get a better view of the rivet. The blank part takes practically no stress.

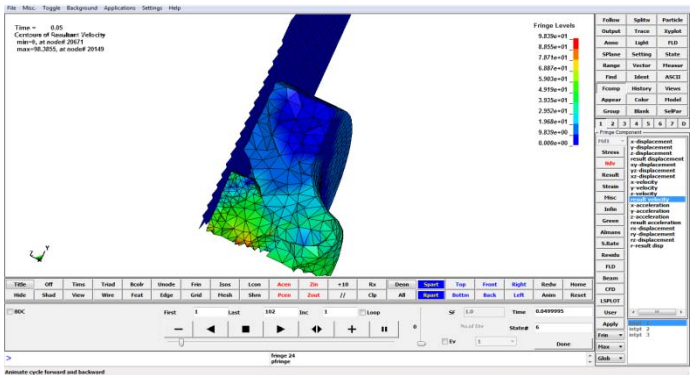

Fig.8. Contours of Resultant Velocity

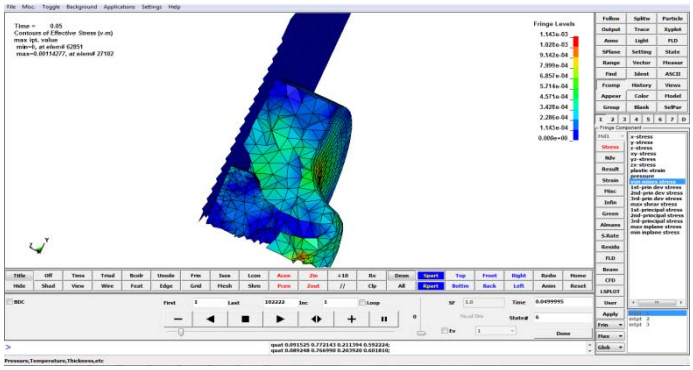

Fig.9. Contours of Effective Stress

Failure is defined as the instant of complete separation of the parts in the model. Fig.9. represents a plots from LS- Dyna, showing the resultant effective stress. The joint is disintegrated by the top-sheet peeling itself over the rivet. For the resultant velocity cases the blank part is removed to get a better view of the rivet. Meshed part is shown above in figure and can see fringe levels, in fringe level different stress at different occasion. The blank part takes practically no stress.

4.1Energy

The energy (total) in the model, which also can be named external work, is composed of different energies. The various energies are shown. In this work, the energy is expressed in pascal.

1. Total energy dissipated through frictional effects,
2. Kinetic energy,
3. Energy dissipated by rate-independent and rate-dependent plastic deformation.
4. Artificial" strain energy associated with constraints used to remove singular Modes (such as hourglass control) and
5. Other energies.

The energy magnitudes are shown in fig.10.

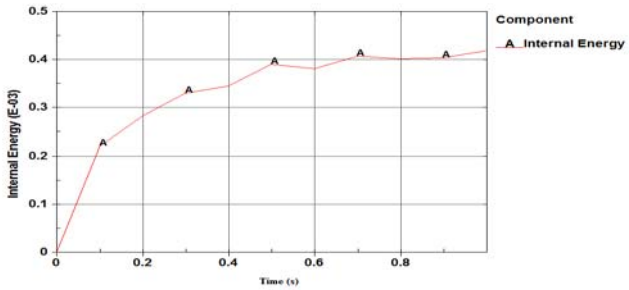

Fig.10. Internal Energy vs Time

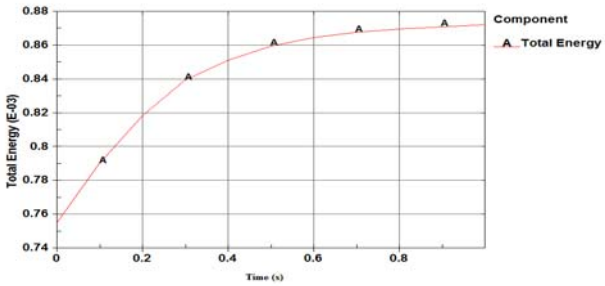

Fig.11. Total Energy vs Time

The kinetic energy curve shows a typical dynamic response result with the oscillating variations.

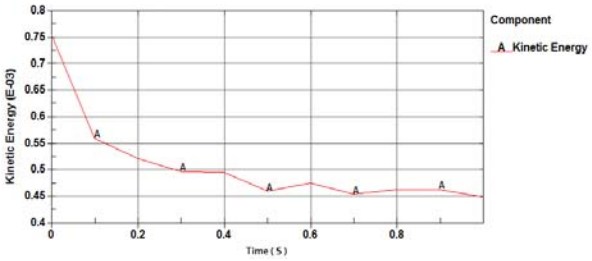

Fig.12. Kinetic Energy vs Time

The external work is 1-2 % larger than the integrated energy due to rounding error and accuracy. The integrated value should be the most accurate. The total energy mostly consists of the plastic deformation energy. When a plateau is reached, failure in the joint has occurred, i.e. no more energy is added to the model. When the energy curve drops, in the beginning, it indicates that the load has changed direction during the deformation lapse.

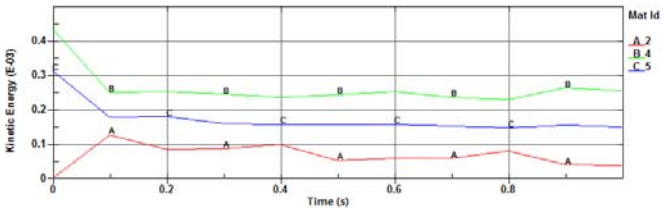

Fig.13. Total Kinetic Energy vs Time

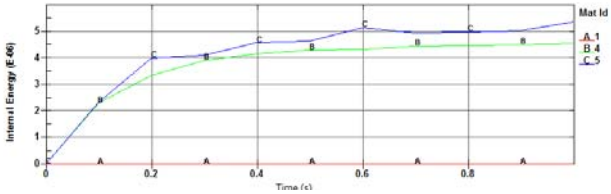

Fig.14. Total Internal Energy vs Time

4.2 Velocity

In this chapter different velocities are simulated. The applied velocity load is not equal to the velocity of the car. In fact in most cases the car velocity is much higher than the velocity that affects the joint, due to different kind of damping in the car structure.

The velocity has a significant influence on the structural dynamic response. One cause is that the material behaves differently as the strain rate changes with velocity.

The oscillations are dependent of the acceleration of the applied velocity load. As it is applied instantaneously it creates a very high acceleration, which starts a longitudinal transient chock wave. This wave propagates back and forth through the specimen. The damping in the model decreases the amplitude until the oscillating disappears.

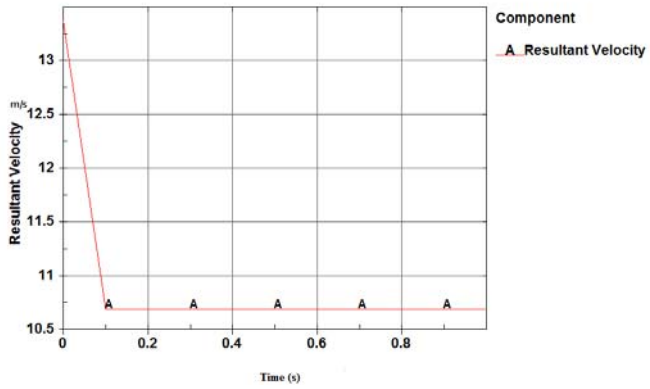

Fig.15. Resultant Velocity vs Time

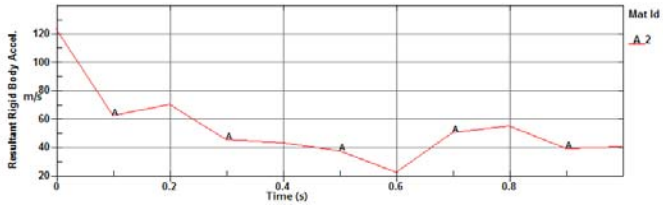

Fig.16. Resultant Rigid Body Acceleration vs Time

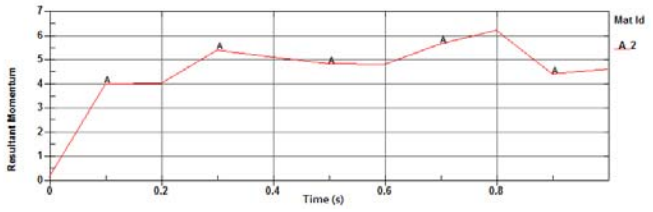

Fig.17. Resultant Momentum vs Time

5. Conclusion

It was found that:

1. When making a finite element model, a number of parameters can be changed or introduced. This makes it time-consuming and difficult to get the most suitable model.
2. All the cases studied shows a model deformation process with the top sheet peeling itself over the rivet head and cause by that a failure in the model.
3. Higher velocity results in higher load levels, higher energy and therefore also larger failure displacement.
4. The deformation process was more or less similar. For these cases the rivet and the bottom sheet around it is quite still.
5. Direct application of the velocity load gives very large peak loads, which isn't a realistic behavior.

REFERENCES

1. Xiaocong He, "Influence of Sheet Material Characteristics on the Torsional Free Vibration of Single Lap-jointed Cantilevered SPR Joints", International Conference on Measuring Technology and Mechatronics Automation, pp 800-805, 2009,
2. Liu Ruijun, "Weight analysis on parameters of self-pierce riveting", international journal of Materials Processing Technology, pp. 1892-1895, 2011,
3. Shoichiroyoshihara, Hisashi Nishimura et al., "Effect of blank holder force control in deep – drawing process of magnesium alloy sheet", 2005 Journal of Material Processing Technology, Japan, pp 579 -585, 3 june 2005.
4. Naoki Sakamoto, Mitsuru Higashimori et al., "Piercing Based Grasping by Using Self-Tightening Effect", 2008 IEEE International Conference on Robotics and Automation Pasadena, Mayekawa Mfg. Co., Ltd., CA, USA, pp. 4056-4060,, May 19-23, 2008.
5. Liu Ruijun, Dang Xiangwen "Mechanical behaviour of self-piercing riveted two-layer joints with different surface treatment",. 2011 International Conference on Mechatronic Science, Electric Engineering and Computer, Jilin, China, pp. 703 -706, August 19-22, 2011.
6. Schwer et al., "An Assessment of the LS-DYNA Hourglass Formulations via the 3D Patch Test'', 5th European LS-DYNA Users Conference, Livermore Software and Technology Corporation, Livermore CA, April 2003.
7. Robert W. Bielenberg et al., Modeling crushable foam for the safer racetrack barrier" 8th International LS-DYNA Users Conference, New Energy-Absorbing High-Speed Safety Barrier, " Transportation Research Record, pp. 6.1-6.10, November 2003.
8. Martin S. Annett "Analysis of a Full-Scale Helicopter Crash Test" Structural Dynamics Branch, 11th International LS-DYNA Users Conference, Special Issue on Ballistic Impact and Crashworthiness of Aerospace Structures, pp. 7.1-7.10, December 2009.
9. Benhizia, T.Outtas, " Numerical Simulation of Frontal Offset Crash Test for the Vehicle Frame using Ls Dyna", World Academy of Science, Engineering and Technology 79, *pp. 10-15,* 2011.
10. Ying Yang, GuangyaoZhao_Jianwei Di, "Analysis of Vehicle's Frontal Crash Based on Structures' Section Forces", 8th Internationl LS-DYNA Users Conference, pp. 83-95, 2004
11. S. D. Rajan, B. Mobasher and A. Vaidya, "Implemented Multi-Layer Fabric Material Model Development for Engine Fragment Mitigation", 11 th International LS-DYNA Users Conference, Arizona State University, pp no 47 -56, 2006.
12. Xin Sun and Mohammad A. Khaleel, "Performance Optimization of Self-Piercing Rivets Through Analytical Rivet Strength Estimation", Pacific Northwest National Laboratory, Journal of Manufacturing Process, Vol. 7/No. 1, pp no 83 – 95, 2005.

13. Himanshuv.Gajjar, Anish H.Gandhi, and Harit k Raval, "Finite Element Analysis of sheet Metal Air bending using Hyperform LS-DYNA". Engineering, pp no:117-122, 2007.
14. John O. Hallquist, L S- DYNA Theory manual, March 2006.